Technology for Seamless Multi-Projection onto a Hybrid Screen Composed of Differently Shaped Surface Elements

Masami Yamasaki[1], Tsuyoshi Minakawa[1], Haruo Takeda[1], Shoichi Hasegawa[2], and Makoto Sato[2]

[1]Systems Development Laboratory
Hitachi Ltd.
1099 Ohzenji, Asao-ku
Kawasaki, 215-0013 Japan
{yamasaki,mint,takeda}@sdl.Hitachi.co.jp

[2]Precision and Intelligence Laboratory
Tokyo Institute of Technology
4259 Nagatsuta, Midori-ku
Yokohama, 226-8503 Japan
{hase,msato}@pi.titech.ac.jp

Abstract

We describe a tiled-projection display system whose entire image is composed of twenty four patches of projection, sixteen of which are used for front projection and eight of which are used for rear projection on the center area of the screen. Eight pairs of the projectors are used to project stereoscopic images, the left-eye image and the right-eye image. The screen consists of differently shaped surface elements that are the partial surfaces of such objects as planes, spheres, cylinders and tori.

The following three technologies were developed for the display system: (1) a digital camera based measurement of the position and the color features of the pixels projected on a screen, (2) software that computes the geometry correction and the color modulation for edge blending by using the measurement data, and (3) real time image processing hardware to enable arbitrary geometrical warping and color modulation for individual pixels.

1. Introduction

Covering an audience's whole field of view with as many projectors as possible is a simple but good idea to provide an immersive viewing experience. The quality of such a projection-based tiled display depends on how well an invisible seam is achieved between the adjacent image patches that constitute a whole image with a correct shape. For the purpose of integrating image tiles into a seamless whole, edge blending, projection alignment, and calibration are major technical challenges.

Edge blending is necessary for smooth transition between adjacent images projected on a screen. In order to modulate appropriately the intensity of the image in the overlapped region of projected images, there are two techniques. One is optical shading in the overlapped region by using physical shadow masks [1]. The other is modification of the source image provided to projectors by using software or hardware [2].

Geometry correction for tiled-projection display systems is necessary for two reasons. One is that edge blending needs correct alignment of corresponding pixels projected from multiple projectors in the overlapped projection region on a screen. The other is to control the intended shape of the whole projected image. Such geometry correction is achieved by distorting the image with software or hardware.

Software to distort the image so that projected pixels are aligned correctly on the screen has been developed [3][4]. The capability to distort images is very essential in the case of building a tiled-projection display system with projectors whose image device is an LCD or DMD, which has no capability to distort images in contrast to a CRT. Image processing hardware is a very attractive approach to avoid the performance problem accompanying the software approach. Recently some companies began shipping image-processing hardware that has both edge blending and geometry correction capabilities.

To manually produce the image warping parameters for geometry correction and the modulation patterns for edge blending is a time consuming task. To manually determine optimal parameters for a system in which images are projected on a curved screen is actually impossible. For a curved screen, the parameters need to be computed from the positional information of the projected pixels on the screen and the pixels' luminous property [4][5][6][7].

In the following section, we describe an immersive projection system that has a screen composed of complex surface elements. The surface elements of the screen were derived from various geometrical objects such as planes, spheres, cylinders and tori. To cover

the entire surface of the screen with projection images, sixteen projectors were used with additional eight projectors for rear projection on the center area of the screen. We also describe how we computed geometry correction parameters and edge blending parameters based on measurement of the pixels projected on the screen by using a digital camera.

2. System Organization

The display system we developed was designed as a visual component of a system that provides a virtual experience with physical force feedback brought about by a wire driven force display subsystem [8] and a locomotion interface subsystem using a computer controlled turntable.

Our screen design attempted to satisfy the following four conditions: (1) to completely cover a viewing area, (2) to extend its size as far as possible within the limit of the space available, (3) to make the shadow cast by the viewer as small as possible, and (4) to enable stereoscopic image projection.

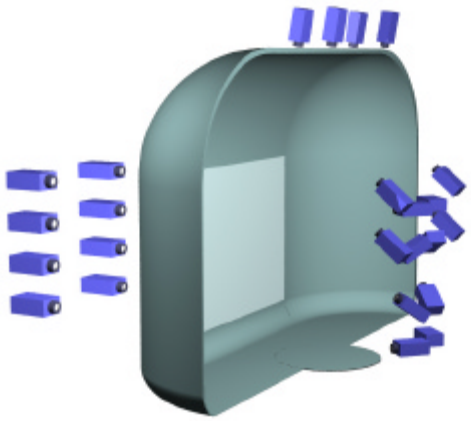

Figure 1. The hybrid screen composed of differently shaped surface elements and twenty four projectors installed to cover the entire surface of the screen.

As shown in Fig. 1, the resultant screen is 6.3 meters wide, 4.0 meters high, and 1.5 meters deep. The central flat part of the screen is for rear projection with eight projectors with SXGA, 1280x1024 pixels, resolution. The remaining part of the screen is for front projection with sixteen projectors of XGA, 1024x768 pixels, resolution. The projectors were set up at the positions indicated in Fig. 1, and Fig. 2 shows the projectors for front projection mounted on posts. Figure 3 shows the position where the viewer stands when a virtual reality environment is provided.

As previously mentioned, the screen is composed of partial surfaces of planes, spheres, cylinders, and tori, as shown in Fig. 4. Such a uniquely shaped screen is made of fiberglass reinforced plastic (FRP) that has not only capability to reproduce complex shape but also enough rigidity to support itself.

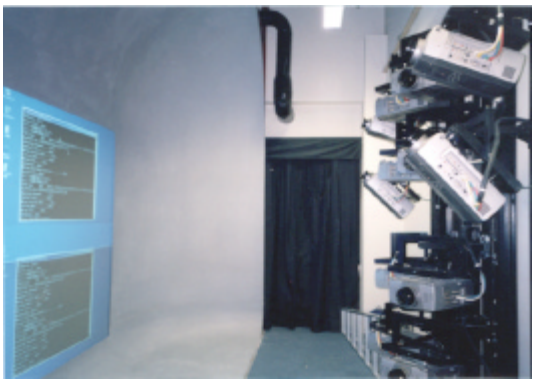

Figure 2. The front side view of the display system.

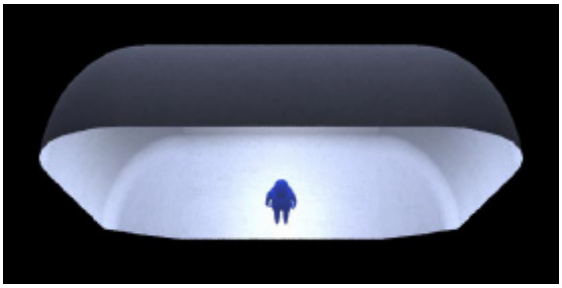

Figure 3. The position for the viewer when a virtual reality environment is provided.

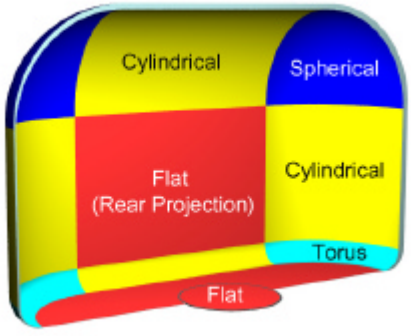

Figure 4. The various surface elements that constitute the entire surface of the screen.

Eight pairs of projectors are used to project stereoscopic images, the left-eye image and the right-eye image, onto the rear projection screen and the upper and lower cylindrical parts of the front projection screen. We used orthogonal linear polarized lights to project each image for the left and the right eye. To maintain the light polarization after it is diffused onto the front projection screen, we painted the front screen with gray paint mixed with aluminum powder. The rear projection screen is suitable for conserving polarization of light and has a rather high gain.

A high gain screen for rear projection diffuses the stronger light more parallel to the incoming light's direction than to other directions. This property is not suitable for edge blending because the blending ratio for incoming light from different directions depends on the viewing angle of an observer. However, we used a high gain screen because for us it was more important to use a stereoscopic display system.

The video images provided to the projectors were generated by twenty four PC's that were inter-connected by a fast (2.0 Gbps) network. A UDP-based network software mechanism synchronized each frame of the video images. The video output from each PC was not directly supplied to projectors, but rather the video signal went through image processing hardware that worked as a filter to geometrically warp and modulate the color of the image encoded in the video signal.

3. Geometry Correction

The purpose of geometry correction for the projection images is to achieve a desired shape whole and complete on the screen. Therefore, to derive the parameters of the image distortion for the geometry correction, we must first decide the shape to be projected on the entire screen. Our intended projection is a perspective projection onto the screen surface from a lens center located one meter from the eye position of the viewer(Fig. 3). Indeed, the best position of the lens center for a perspective projection is the same position as the eye position of the viewer. However, the positioning of the lens center one meter behind the viewer eye position was necessary for using a digital camera with a fish-eye lens to measure the position of the pixels projected on the screen. We call the lens center the system viewpoint in the following description.

We measured the position of pixels on the screen by using two different ways to compute the geometry correction. First, we measured the direction of pixels projected on the screen from the fixed viewpoint corresponding to the system viewpoint of our intended perspective projection mentioned above. Second, we measured the relative positional relation between pixels projected in the overlapped area from different projectors by taking a close-up photo from appropriate viewpoints. A second type of information was created for every pair of projectors whose projection image overlapped on the screen.

The first type of measurement was done by using a digital camera with a fish-eye lens. This directional information of pixels from a fixed viewpoint was sufficient to correct the whole shape of the projected image, but it was not accurate enough to achieve subpixel alignment in overlapped regions for fine edge blending. Therefore, a second measurement was necessary for the subpixel alignment.

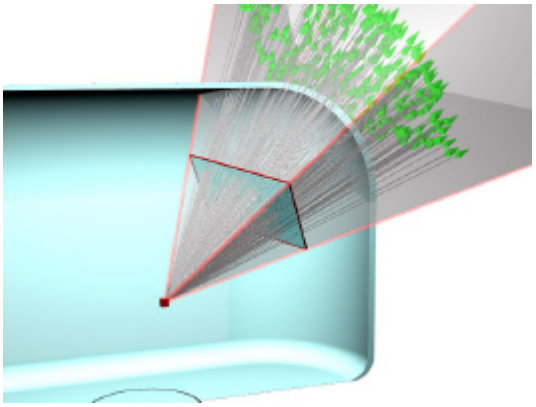

Figure 5. The measured direction vectors of pixels of the projector that projects an image onto the upper right corner of the screen and the view volume of the corresponding virtual camera.

Even though rendering performance of the PC is growing year by year, it is not fast enough to render perspective projections onto a curved surface. For this reason, we assumed that an image fed to each projector through image-processing hardware was rendered based on a perspective projection onto a flat film surface. An appropriate camera parameter for the perspective projection for rendering an image was chosen based on their view volume's ability to cover the direction vectors of pixels on the screen from the system viewpoint we mentioned above. Figure 5 shows the distribution of the direction vectors of pixels of the projector that projected an image onto the upper right corner of the screen.

We defined a virtual camera for each projector so that the view volume of the virtual camera included almost all pixel direction vectors of the corresponding projector. The boundary of the view volume of the corresponding virtual camera is shown in Fig. 5. All the fields of view of the virtual cameras are shown in Fig. 6. Image data supplied to projectors through image-processing hardware was rendered based on the virtual cameras.

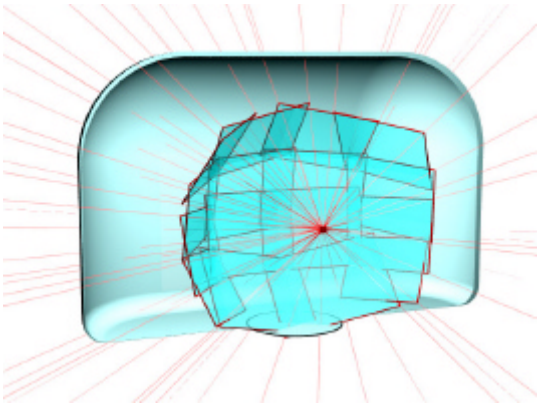

Figure 6. The view volumes and the projection surfaces of virtual cameras defined for every projector.

When the image rendered with the virtual camera was projected from the system viewpoint onto the screen with the same perspective projection parameter as the virtual camera, the correct scene could be generated for a viewer whose viewpoint is that of the system viewpoint. The image projected from the virtual projector can be emulated on the screen with a real projector only within the restricted region that is the intersection of the two projection area on the screen, one from a real projector and another from a virtual projector.

We can define a two-dimensional image warping such that if the image supplied to the real projector is transformed according to the image warping, the projected image on the screen emulates the image projected by the virtual projector.

Let S be a set of pixels of a two dimensional image, and let D be a set of the direction of unit vectors in the three dimensional space. We can define numerically a map f_k:S ->D for the projector k with the measured direction of pixels projected on the screen by the real projector k. Another map g_k:S ->D is defined as an inverse of the perspective projection of the virtual camera corresponding to the projector k.

If we can define a map from pixel to pixel, h_k:S->S , that satisfies the following equation:

$$f_k \text{ o } h_k = g_k$$

the projection of the virtual projector can be emulated by using the image warping defined by h_k. The image warping for the projector that projected an image at the upper right corner of the screen is shown in Fig. 7.

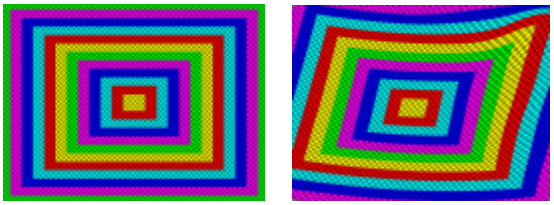

Figure 7. The image warping of the geometry correction for the projector that projected an image at the upper right corner of the screen. The left image is geometrically warped to the right image by the geometry correction.

Since the information of the pixel direction was measured by using a digital camera with fish-eye lens in a fixed pose, it was difficult to keep the information around the view area as accurate as that in the center of the image. Such lost information prevents subpixel accuracy of the pixel positional information.

In order to compensate for the inaccuracy, we measured the relative positional relation between pixels projected in the overlapped area from different projectors by taking a close-up photo from an appropriate viewpoint. The relative positional relation of pixels between projector k and projector m can be represented as a pair of pixel coordinates in the imaging device of each projector, where every pixel of the imaging device of a projector are supposed to be labeled (x,y) where x and y take integer numbers.

The relation {(x,y),(u,v)} between projector k and projector m were such that both the pixel labeled by (x,y) of the projector k and the pixel labeled by (u,v) of the projector m were projected on the same place on the screen. In general, the coordinate components u and v are not integer numbers even if (x,y) has a pair of integer numbers. The floating number coordinate was derived by interpolating the integer coordinates of pixels projected near the position where pixel (x,y) is projected on the screen. Such derived information has subpixel accuracy.

The image warping for the geometry correction derived from the pixel directional information was adjusted with the data of the relative positional relationship of pixels in order to improve the accuracy of pixel alignment in the overlapped region. This adjusted image warping was the final result of the geometry correction.

The data of the relative positional relation of pixels between a pair of projectors to project the stereoscopic view could be used to generate the geometry correction of the image for the one eye from the same geometry correction for the other eye. Thus, the geometric correction for the image for more than one eye was not computed. Such a transformation using the relative positional relation of pixels between a pair of the projectors for stereoscopic view was also used to generate the edge blending pattern for the one eye from the same edge blending pattern for the other eye.

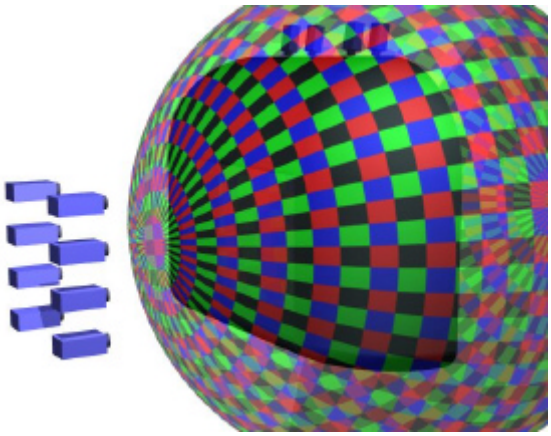

Figure 8. A virtual checker-painted spherical object with the screen and the projectors.

In order to see how well the geometry correction worked, we displayed an image of the scene in which we look at a sphere from the center of the sphere. The surface of the sphere was painted with the checker pattern generated by the circles of every five-degree of longitude and latitude, and the sphere was rotated so that the pole axis of the sphere object was perpendicular to the rear projection screen. The sphere object is supposed to be located as shown in Fig. 8. The image data supplied to each projector through the image processing hardware was rendered in the scene including only the sphere shown in Fig. 8 by using the virtual camera parameter. After the rendered image was distorted according to the geometry correction by using the image processing hardware, the final image was projected on the screen. We took photographs of the screen on which the sphere image was displayed. The photograph in Fig. 9 was taken with a normal lens. The photograph in Fig. 10 was taken with a fish-eye lens from the center of the virtual sphere object. Since the circles of the latitude are reproduced correctly, we can say that the geometry correction worked successfully.

If the computation of the geometry correction is based on such a measurement as described in this section, the margin of error for the construction of the display system is not required to be the smallest. The rigidity of the mechanical components of the system is only required after the system is set up.

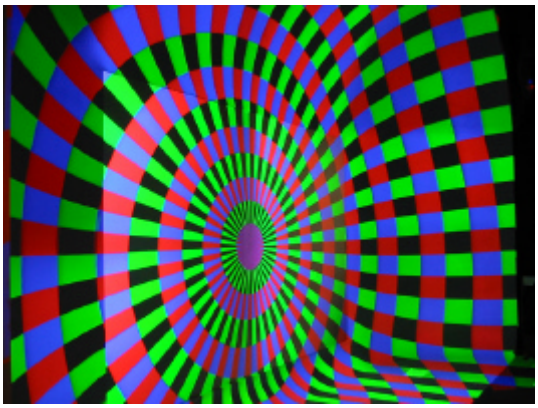

Figure 9. The screen on which a virtual spherical object is displayed with the geometry correction.

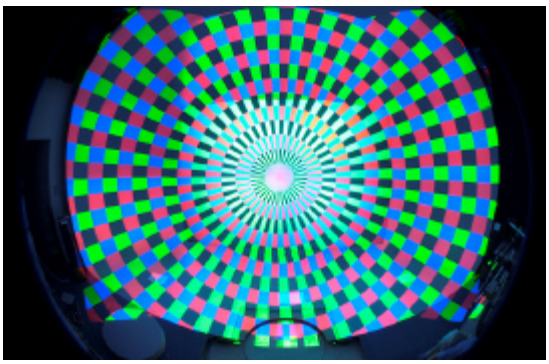

Figure 10. A photograph taken with a fish-eye lens from the center of the displayed spherical object.

4. Edge Blending

To generate an edge blending pattern by hand when the shape of the overlapped region is not a simple

rectangle is difficult. The shape of the overlapped region on the front projection screen can be seen in the photograph in Fig. 11. Even though the photograph is distorted in the unique manner of the fish-eye lens, we can see that the overlapped regions have triangular, round-edged rectangular, or polygonal shapes. The computation of the edge blending patterns for such an irregular shaped overlapped region was based on the relative positional relationship of pixels. The computed edge blending pattern is shown in Fig. 12.

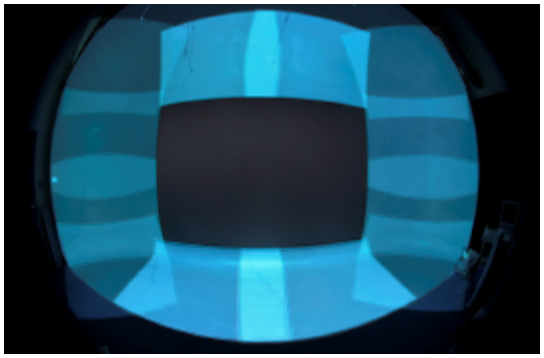

Figure 11. A fish-eye photograph of the front projection screen on which images are projected with overlaps.

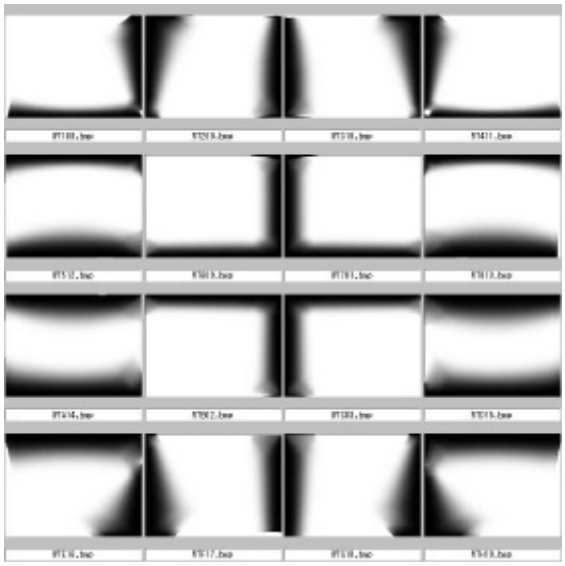

Figure 12. The computed edge blending patterns. Each edge blending pattern is arranged with the same positional relationship of each projection image in Fig. 11. The central four patterns are for the rear projectors that are not shown in Fig. 11.

The edge blending pattern depends on a geometry correction because a finite blending ratio cannot be assigned to a pixel with a position not transformed according to the geometry correction. Thus, we must first compute the geometry correction before computing the edge blending pattern.

The computation of the intensity modulation function for each pixel in the overlapped area was based on a measurement of the color features of the projected pixels. The color features ware measured by using a calibrated digital camera with a fish-eye lens. The color feature measured depended on the view position of the camera because of the high screen gain that was necessary for a stereoscopic image. Therefore, the best blending result was observed only from the viewpoint from which color feature was measured.

The front-projected images were blended smoothly with the adjacent front-projected images. The rear-projected images were blended smoothly only with adjacent rear-projected images. Between the front-projected image and the rear-projected image, we did not attempt smooth edge blending because there were no effective overlapped regions to blend. The rear-projected image was masked by the frame of the central rectangular opening of the front projection screen. An image front-projected onto the rear projection area of the screen cannot be seen from the viewing side.

5. Image Processing Hardware

We developed image processing hardware for the geometry correction and edge blending. This hardware enables the real time processing of any type of geometrical warping and the color modulation of individual pixels.

The geometrical warping was done as an inverse mapping with bilinear interpolation. The parameters for the geometrical warping was stored as a table of the coordinates of the source pixels for every pixel of the output image data. We could set the coordinate of a source pixel with subpixel resolution of four bits. In order to support arbitrary mapping, we needed random access to the input frame. Hence, the input image was alternately buffered to a dual port frame memory. While filling one frame memory, pixel data were read from another frame memory according to the table of coordinates for the inverse mapping.

Color modulation for individual pixels was necessary not only for the edge blending but also for correcting the color uniformity of the projected image. The color modulation function was specified with a segmented linear function with nine vertices. The

color modulation was applied to the color data of the pixels that were generated in the previous inverse mapping module.

We show the block diagram of the image-processing hardware in Fig. 13. The color data of a pixel has twenty four bits at the output of the video signal input interface block. After converting twenty-four-bit color data to thirty-bit color data with the look-up table, LUT0, the thirty-bit computation accuracy can be maintained in the data processing of the geometrical warping and the color modulation. The look-up table, LUT0, is used so that the color data are proportional to the physical intensity of the light. This processing is necessary to get a correct anti-alias result with the bilinear interpolation.

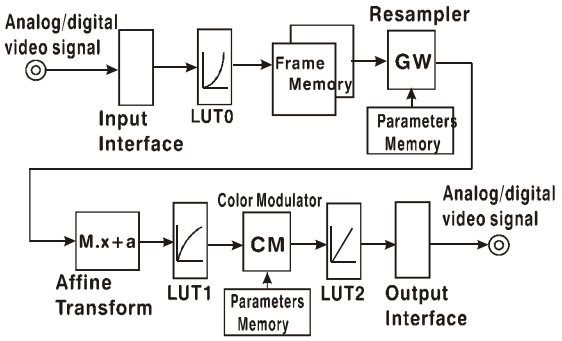

Figure 13. The block diagram of the image-processing hardware.

(a)

(b)

Figure 14. Image-processing hardware. (a) Model PA99. (b) Model PA21.

The output color data from the inverse mapping block can be transformed with a three dimensional affine transformation and the look-up table, LUT1 as the constant color modulation for every pixel. The color modulation block applies individual modulation functions to every pixel. After being transformed by the look-up table, LUT2, the color data are converted to video signals.

We have developed two models, PA99 and PA21, both of which were used for the display subsystem described in this paper. These were implemented as full size modules for the PCI bus as shown in Fig. 14. Model PA99 was developed in 1999 with the maximum pixel frequency of 65 MHz that corresponds to 60 frames of XGA image per second. The maximum pixel frequency of the model PA21 is 130 MHz, equal to the pixel rate of 60 frames of SXGA image per second. Both models have an analog video signal interface for input and output. Model PA21 can handle digital video signals through the DVI interface.

6. Conclusion

We developed the following three technologies for an immersive projection display: (1) a digital camera based measurement of the position and the color features of the pixels projected on a screen, (2) software that computes the geometry correction and the color modulation for edge blending from measurement data, and (3) real time image processing hardware to enable arbitrary geometrical warping and color modulation for individual pixels.

These technologies were used to build a display system whose entire image is composed of sixteen patches of front projection and additional eight patches for rear projection in the center of the screen area. Eight pairs of the projectors are used to project stereoscopic images, the left-eye image and the right-eye image. The screen consists of differently shaped surface elements that are partial surfaces of such objects as planes, spheres, cylinders and tori.

A desired geometry correction to reproduce the desired image from a presumed viewpoint was successfully computed from the measurement of pixel positions. If the computation of the geometry correction is based on the measured positional information of pixels on the screen, the margin of error for the construction of the system is not required to be the smallest. The rigidity of the mechanical components of the system is only required after the system is set up.

7. References

[1] K.Li and Y.Chen, "Optical Blending for Multi-Projector Display Wall System," Proc. 12th Lasers and Electro-Optics Society 1999 Ann. Mtg., IEEE Press, Piscataway, N.J., Nov. 1999.

[2] T. Mayer, "Design Considerations and Applications for Innovative Display Options Using Projector Arrays," SPIE Proc.,Vol.2650:Projection Displays II,M.H.Wu, ed.,SPIE, Bellingham, Wash. 1996, pp. 131-139.

[3] R. Rasker et all., "Multi-Projector Displays Using Camera-Based Registration," Proc. of IEEE Visualization 1999, ACM Press, New York, Oct. 1999.

[4] R. Rasker et al., "The Office of the Future: A Unified Approach to Image-Based Modeling and Spatially Immersive Displays," Proc. Siggraph 98, ACM Ann. Conf. Series, ACM Press, New York, 1988, pp. 179-188. Future office.

[5] R. Surati, Scalable Self-Calibrating Display Technology for Seamless Large-Scale Displays, PhD thesis, Dept. of Electrical Engineering and Computer Science, Massachusetts Institute of Technology, Cambridge, Mass., 1999.

[6] Y. Chen et al., Methods For Avoiding Seams On High-Resolution Multi-Projector Displays Using An Uncalibrated Camera, Tech. Report TR-618-00, Dept. of Computer Science, Princeton Univ., N.J., April 2000.

[7] H. Takeda et al.,"A Video-based Virtual Reality System," ACM VRST '99, pp.19-25, London, UK, Dec. 1999.

[8] L. Buoguila, et al.,"New Haptic Device For Human Scale Virtual Environment: Scaleable-SPIDAR", ICAT'97, pp.93-98, Tokyo, Dec. 1997.